This article was downloaded by:[Max Planck Inst & Research Groups Consortium]
[Max Planck Inst & Research Groups Consortium]
On: 15 June 2007
Access Details: [subscription number 771335669]
Publisher: Taylor & Francis
Informa Ltd Registered in England and Wales Registered Number: 1072954
Registered office: Mortimer House, 37-41 Mortimer Street, London W1T 3JH, UK

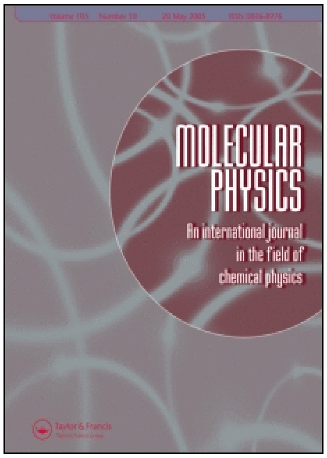

Molecular Physics
An International Journal in the Field of Chemical Physics
Publication details, including instructions for authors and subscription information:
http://www.informaworld.com/smpp/title~content=t713395160

Packing effects on the conformational equilibrium of alkanes

P. Padilla [a]; C. Vega [b]
[a] Chemistry Laboratory, III, HC Ørsted Institute. Copenhagen 0. Denmark
[b] Departamento de Quimica Fisica, Facultad de Ciencias Quimicas, Universidad Complutense. Madrid. Spain

To cite this Article: Padilla, P. and Vega, C. , 'Packing effects on the conformational equilibrium of alkanes', Molecular Physics, 84:2, 435 - 450
To link to this article: DOI: 10.1080/00268979500100291
URL: http://dx.doi.org/10.1080/00268979500100291

PLEASE SCROLL DOWN FOR ARTICLE

Full terms and conditions of use: http://www.informaworld.com/terms-and-conditions-of-access.pdf

This article maybe used for research, teaching and private study purposes. Any substantial or systematic reproduction, re-distribution, re-selling, loan or sub-licensing, systematic supply or distribution in any form to anyone is expressly forbidden.

The publisher does not give any warranty express or implied or make any representation that the contents will be complete or accurate or up to date. The accuracy of any instructions, formulae and drug doses should be independently verified with primary sources. The publisher shall not be liable for any loss, actions, claims, proceedings, demand or costs or damages whatsoever or howsoever caused arising directly or indirectly in connection with or arising out of the use of this material.

© Taylor and Francis 2007

MOLECULAR PHYSICS, 1995, VOL. 84, NO. 2, 435–450

Packing effects on the conformational equilibrium of alkanes

By P. PADILLA
Chemistry Laboratory, III, HC Ørsted Institute, Universitetsparken 5, DK-2100
Copenhagen 0, Denmark

and C. VEGA
Departamento de Quimica Fisica, Facultad de Ciencias Quimicas, Universidad
Complutense, 28040 Madrid, Spain

(*Received 2 August 1994; revised version accepted 12 October 1994*)

The equation of state and the conformational equilibrium of repulsive models of n-hexane, n-heptane and n-octane are investigated by the method of molecular dynamics simulation. For repulsive models the simulation results show that the conformational population at liquid densities differs from that of the gas. Packing effects enhance the population of chains in more spherical conformations, which are in general those presenting a large fraction of bonds in the *gauche* state. Good agreement is found when comparing the simulation data with a recently proposed equation of state for hard n-alkanes models. Furthermore, the theory predicts correctly the shift in the conformational equilibrium due to packing effects. The role of attractive forces on the conformational equilibrium is also discussed. It is found that attractive and repulsive forces favour different kinds of conformers at high densities. This explains why the conformational equilibrium of n-alkanes at liquid densities does not differ significantly from that of the gas. The present simulation data may be useful for testing different theoretical treatments recently proposed for hard n-alkane models.

1. Introduction

During the last decade, a great amount of effort has been devoted to the study of molecules with internal flexibility. Computer simulation studies of flexible chain models either by Monte Carlo (MC) or by molecular dynamics (MD) have appeared [1–9]. From a theoretical point of view, interest has focused on the determination of an equation of state (EOS) for hard flexible models. It is expected that the attractive forces may be incorporated in a perturbative way. Four different theoretical approaches have been developed: integral equation theory [10], an extension of the Flory theory to hard flexible models [11], density functional theory [12, 13] (which has also been applied to these kinds of molecules) and, finally, Wertheim's theory of association, which has been extended to allow for the study of hard flexible molecules [14–16]. The tangent hard spheres model [17] has attracted most attention. Although this is an interesting model, it is not realistic for real chain molecules like n-alkanes. Following the work of Boublík *et al.* [18], one of us has recently modified the EOS proposed by Wertheim [14] and Chapman *et al.* [15] for the tangent hard spheres model, and developed a theory that allows for overlap of the hard spheres constituting the molecule [19]. That provides a more realistic description of real chain molecules. The proposed theory permits us to analyse the role of density on the conformational equilibrium. Although some comparison between this theory and simulation data has been done already for butane and pentane, with satisfactory agreement [19], the ability of the theory to describe the EOS for longer chains remains untested. This is also the case for the theoretical predictions concerning the effect of density on the conformational equilibrium.

In this work we present results from MD simulations for repulsive models of n-alkanes. The equation of state and the populations of the different conformers are obtained for several chain lengths at different densities. These simulation data may be useful for testing the different theoretical approaches presented so far for hard flexible models. In particular, we compare the simulation results with the predictions of the modified Wertheim treatment proposed recently [19].

2. Simulation methodology

The model studied is similar to that of Ryckaert and Bellemans [1]. Each methylene or methyl group is modelled as a single site placed at the position of the carbon nucleus. The masses of both the methylene and methyl groups are made equal, and set to $2{\cdot}41 \times 10^{-26}$ kg. The bond distance is fixed to $l = 1{\cdot}53$ Å by imposing holonomic constraints [20]. The value of the equilibrium bond angle CCC is $\theta_e = 109{\cdot}5°$. Most of the simulations of this work were made with the bond angles fixed to their equilbrium values by imposing holonomic constraints. This model with fixed bond angles will be denoted as the rigid model (RM). In order to understand the role of bond angle vibrations on the equation of state and conformational equilibrium, a few simulations were made using the following bending potential:

$$u_b(\cos\theta) = \tfrac{1}{2}k_\theta(\cos\theta - \cos\theta_e)^2, \qquad (1)$$

where θ is the current value of the CCC angle and k_θ is the force constant. Two values of k_θ were considered, namely 520 kJ mol^{-1} and 1040 kJ mol^{-1}. This model with bond angle vibrations will be denoted as the flexible model (FM). In all the cases, the torsional potential used in the simulations is that proposed by Ryckaert and Bellemans [1], which will be denoted as u_{RB}. Intermolecular and intramolecular interactions are given by a Weeks–Chandler–Anderson (WCA)-like potential [21]:

$$u^{WCA} = 4\epsilon\left(\left(\frac{\sigma}{r}\right)^{12} - \left(\frac{\sigma}{r}\right)^{6}\right) + \epsilon \qquad r < 2^{1/6}\sigma, \qquad (2)$$

$$u^{WCA} = 0 \qquad r > 2^{1/6}\sigma. \qquad (3)$$

with $\epsilon/k = 72$ K and $\sigma = 3{\cdot}923$ Å. Intramolecular interactions as given by equations (2) and (3) are included only between carbons separated by more than three CC bonds. In all the systems studied, the value of the temperature was $T = 366{\cdot}88$ K. At this temperature, the Barker–Henderson prescription [22] for determining the equivalent hard core diameter d gives $d = 3{\cdot}7109$ Å. Therefore, the reduced bond length is $L^* = l/d = 0{\cdot}4123$, which corresponds to the model studied previously [19]. At this temperature, it is expected that the results for the WCA potential should be close to those of a hard model with this reduced bond length. During the simulation, the temperature was kept constant with the help of a Nosé–Hoover thermostat [23], and the equations of motion were solved with the leap-frog algorithm [24]. In all the cases, the simulation sample was composed of 64 chains. The molecules were contained in a cubic box with periodic boundary conditions. The timestep was set to 1·0 fs. A typical time for equilibration was 40 ps, and after that the simulation run length was of 1200 ps. Subaverages were collected every 120 ps. The results presented for the simulations are the averages of the subaverages. The uncertainty was estimated as the standard deviation.

The use of MD for sampling the configurations of chain molecules at low densities in order to obtain the ideal gas population of conformers is not appropriate. Without the randomizing effect of molecular collisions, conformational relaxation times become much longer at lower densities compared with melt densities. Thus the precision of the fraction of conformers diminishes for a given simulation time. Because of that, the use of MC algorithms to compute ideal gas populations seems preferable. In this work MC integration was performed in order to compute the distribution of conformers at zero density (ideal gas population). Details of the calculations are given in section 3.

3. Theory

In addition to the MD results, we present results from a theory proposed recently for hard n-alkane models. This theory is explained in detail in [19]. In this section, we shall describe how the theory is implemented in order to allow for a comparison with the simulation results, either for the RM or for the FM. Let us start with the ideal gas population of the rigid model. In the RM, the mol fraction x_i of a conformer i is given by [2]

$$x_i^{\mathrm{RM}} = \frac{\int_{\Delta i} \exp\left(-\beta(U_{\mathrm{tor}}(\Phi) + U_{\mathrm{WCA}}(\Phi) - 0{\cdot}5kT\ln(H^{\mathrm{RM}}(\Phi)))\right) \mathrm{d}\Phi}{\int \exp\left(-\beta(U_{\mathrm{tor}}(\Phi) + U_{\mathrm{WCA}}(\Phi) - 0{\cdot}5kT\ln(H^{\mathrm{RM}}(\Phi)))\right) \mathrm{d}\Phi} \tag{4}$$

where $\beta = 1/kT$, H^{RM} is the determinant of the metric tensor, U_{WCA} is the intramolecular energy of the molecule due to the WCA potential, Φ is the set of torsion angles defining the conformation of the molecule, U_{tor} is the torsional energy of the molecule, and Δ_i is the domain of torsional angles where the conformer is defined. The torsional energy U_{tor} is given by

$$U_{\mathrm{tor}}(\Phi) = \sum_k u_{\mathrm{tor}}(\phi_k), \tag{5}$$

where $u_{\mathrm{tor}}(\phi_k)$ is the torsional energy due to kth torsion angle. We shall apply the rotational isomeric state (RIS) approximation [25] to the U_{WCA} and to the determinant of the metric tensor. Moreover, we shall perform a summation over equivalent conformers (for instance, in pentane the tg^+ and tg^- are equivalent and we shall denote them as tg). In this way, equation (4) can be rewritten as

$$x_i^{\mathrm{RM}} \simeq \frac{\Omega_i \exp\left(-\beta(U_{\mathrm{WCA}}(\Phi_e^i) - 0{\cdot}5kT\ln(H^{\mathrm{RM}}(\Phi_e^i)))\right) \int_{\Delta i} \exp\left(-\beta(U_{\mathrm{tor}}(\Phi))\right) \mathrm{d}\Phi}{\sum_i \Omega_i \exp\left(-\beta(U_{\mathrm{WCA}}(\Phi_e^i) - 0{\cdot}5kT\ln(H^{\mathrm{RM}}(\Phi_e^i)))\right) \int_{\Delta i} \exp\left(-\beta(U_{\mathrm{tor}}(\Phi))\right) \mathrm{d}\Phi}, \tag{6}$$

where the subscript e denotes the equilibrium configuration of the conformer. For instance, in the conformer tt of pentane, Φ_e denotes the pair of values $\phi_1 = 0$ and $\phi_2 = 0$. The determinant of the metric tensor is also evaluated at the equilibrium configuration by extending the procedure explained in the appendix of [2] to longer chains. In equation (6), Ω_i stands for the degeneracy of conformer i. For instance, in n-pentane the degeneracy of the conformer tg is 4 (tg^+, tg^-, g^+t, g^-t). Now let us define the variable D through the relation:

$$\exp(-\beta D) = \frac{\int_{\pi/3}^{\pi} \exp(-\beta(u_{\mathrm{tor}}))\, \mathrm{d}\phi}{\int_{-(\pi/3)}^{\pi/3} \exp(-\beta(u_{\mathrm{tor}}))\, \mathrm{d}\phi}. \tag{7}$$

The variable D, which has units of energy, represents the effective energy of a *gauche* conformer that provides the correct ratio of *gauche* to *trans* population, as given by the right hand side of equation (7).

By dividing the numerator and the denominator of equation (6) by

$$\int_{\Delta ttt..tt} \exp(-\beta(U_{\mathrm{tor}}(\Phi)))\, \mathrm{d}\Phi, \tag{8}$$

where $\Delta_{ttt..tt}$ represents the domain of torsion angles where the all-*trans* conformation is defined, and using equations (5) and (7), equation (6) can be rewritten as

$$x_i^{\mathrm{RM}} \simeq \frac{\Omega_i \exp(-\beta(U_{\mathrm{WCA}}(\Phi_{\mathrm{e}}^i) - 0{\cdot}5kT \ln(H^{\mathrm{RM}}(\Phi_{\mathrm{e}}^i)) + c_i D))}{\sum_i \Omega_i \exp(-\beta(U_{\mathrm{WCA}}(\Phi_{\mathrm{e}}^i) - 0{\cdot}5kT \ln(H^{\mathrm{RM}}(\Phi_{\mathrm{e}}^i)) + c_i D))}, \tag{9}$$

where the superscript RM means that this equation holds for the rigid model. The integer c_i represents the number of *gauche* bonds in conformer i (for instance $c_i = 1$ for the *tg* conformer of pentane). The value of D is computed easily from the definition, given in equation (7), by substituting the torsional potential, which in this work is the one proposed by Ryckaert and Bellemans ($u_{\mathrm{tor}} = u_{\mathrm{RB}}$). For the temperature studied, $T = 366{\cdot}88$ K, the computed value of D is $3337{\cdot}83$ J mol^{-1}.

For the flexible model, the molar fraction of conformer i is given by

$$x_i^{\mathrm{FM}} = \frac{\int_{\Delta i} \exp(-\beta(U_{\mathrm{tor}}(\Phi) + U_{\mathrm{WCA}}(\Phi, s) + U_{\mathrm{B}}(s) - 0{\cdot}5kT \ln(H^{\mathrm{FM}}(s))))\, \mathrm{d}\Phi\, \mathrm{d}s}{\int \exp(-\beta(U_{\mathrm{tor}}(\Phi) + U_{\mathrm{WCA}}(\Phi, s) + U_{\mathrm{B}}(s) - 0{\cdot}5kT \ln(H^{\mathrm{FM}}(s))))\, \mathrm{d}\Phi\, \mathrm{d}s} \tag{10}$$

where $U_{\mathrm{B}}(s)$ is the total bending energy of the molecule given by the summation over bending angles of a potential of the form of equation (1), s is the set of cosines of the bending angles of the molecule, and $H^{\mathrm{FM}}(s)$ is the determinant of the metric tensor for the flexible model. The appearance of a metric tensor for the flexible model is a consequence of the fact that even in that model the bond length is kept fixed. Note that for the rigid model H is a function of Φ, whereas for the flexible model H is a function of s but not of the torsional angles. The determinant of the metric tensor for the FM can be determined by using a similar approach to that described in the appendix of [2]. For instance, in the case of butane, H is proportional to $8 - \cos^2(\theta_1) - \cos^2(\theta_2)$ [26, 27]. If the value of k_θ is sufficiently large, then only small fluctuations of the bending angles are allowed. In that case, the magnitude of $U_{\mathrm{WCA}}(\Phi, s)$ for a given value of Φ does not change much in the range of allowed fluctuations of the bending angles. Therefore, it is a good approximation to take:

$$U_{\mathrm{WCA}}(\Phi, s) \simeq U_{\mathrm{WCA}}(\Phi, s_{\mathrm{e}}), \tag{11}$$

where s_{e} is the set of cosines of the bending angles at equilibrium (i.e. $s_{\mathrm{e}} = \cos(\theta_{\mathrm{e}})$). By substituting equation (11) into (10), the integration over s uncouples with that over Φ and since it appears in the numerator and denominator of equation (10) it yields unity. Therefore after the approximation of equation (11), equation (10) may be rewritten as

$$x_i^{\mathrm{FM}} \simeq \frac{\int_{\Delta i} \exp\left(-\beta(U_{\mathrm{tor}}(\Phi) + U_{\mathrm{WCA}}(\Phi, s_{\mathrm{e}}))\right) \mathrm{d}\Phi}{\int \exp\left(-\beta(U_{\mathrm{tor}}(\Phi) + U_{\mathrm{WCA}}(\Phi, s_{\mathrm{e}}))\right) \mathrm{d}\Phi}. \tag{12}$$

Now, starting from equation (12) and following a procedure similar to that used for deriving equation (9) from (4), one obtains finally

$$x_i^{\mathrm{FM}} \simeq \frac{\Omega_i \exp\left(-\beta(U_{\mathrm{WCA}}(\Phi_{\mathrm{e}}^i, s_{\mathrm{e}}) + c_i D)\right)}{\sum_i \Omega_i \exp\left(-\beta(U_{\mathrm{WC}}(\Phi_{\mathrm{e}}^i, s_{\mathrm{e}}) + c_i D)\right)}. \tag{13}$$

Equations (9) and (13) yield the ideal gas population within the RIS approximation for the RM and the FM, respectively. Equation (13) shows that for the FM the contribution of H^{FM} to the conformational equilibria can be neglected. By comparing equations (13) and (9) it can be seen that differences between the FM and RM arise only from the presence of H^{RM} in equation (9).

The population of conformers at a density different from zero is obtained following the procedure of [19]. Let us explain how this procedure is implemented for the RM. The free energy of the n-alkane for a given composition of conformers $\boldsymbol{x}$ is defined for the RM by the expression

$$\begin{aligned} A^{\mathrm{RM}}/NkT = {} & \sum x_i \ln(x_i/\Omega_i) + \beta \sum x_i(c_i D + U_{\mathrm{WCA}}(\Phi_{\mathrm{e}}^i) - 0{\cdot}5kT \ln(H^{\mathrm{RM}}(\Phi_{\mathrm{e}}^i))) \\ & + A^{\mathrm{res}}(\boldsymbol{x})/NkT \end{aligned} \tag{14}$$

where A^{res}/NkT is the residual part of the Helmholtz free energy. The residual free energy is obtained from the integration of a modified version of Wertheim's EOS [19]:

$$Z = \frac{p}{\rho kT} = (2\alpha - 1)\frac{1 + y + y^2 - y^3}{(1 - y)^3} - (2\alpha - 2)\frac{1 + y - y^2/2}{(1 - y)(1 - y/2)}, \tag{15}$$

$$A^{\mathrm{res}}(\boldsymbol{x})/NkT = \int_0^{\rho} \frac{Z(\boldsymbol{x}, \rho') - 1}{\rho'} \mathrm{d}\rho'. \tag{16}$$

By substituting equation (15) into (16) one obtains

$$A^{\mathrm{res}}/NkT = 2(\alpha - 1)\ln\left(\frac{2(1 - y)^3}{(2 - y)}\right) - \frac{(2\alpha - 1)(2y - 3)}{(1 - y)^2} - 3(2\alpha - 1), \tag{17}$$

where the average non-sphericity α of the n-alkane and the packing fraction y are defined by

$$y = \rho \sum x_i V_i \tag{18}$$

and

$$\alpha = \sum x_i \alpha_i. \tag{19}$$

In equations (18) and (19) V_i and α_i stand for the volume and non-sphericity parameter of conformer i, respectively, and ρ is the number density. The non-sphericity parameter of conformer i is defined from the relation [28]

$$\frac{B_2^i}{V_i} = 1 + 3\alpha_i, \tag{20}$$

where B_2^i is the second virial coefficient of conformer i. Values of α_i for the different conformers of hard n-alkane models have been reported elsewhere [19]. At each density, the equilibrium composition is obtained by minimizing the free energy with respect to the population of the different conformers. This is equivalent to solving the equations

$$\left(\frac{\delta A^{\mathrm{RM}}/NkT}{\delta x_i}\right) = 0 \tag{21}$$

$$\sum x_i = 1 \tag{22}$$

along with equations (14–20). At low densities, the residual free energy A^{res} goes to zero and the solution of equations (21) and (22) yields equation (9), which is the ideal gas population of the RM. In addition to the conformational population, the equation of state for the density studied is also obtained.

For the FM the free energy of the system is given by equation (14) but without the term involving the metric tensor. The conformational population is obtained again by solving equations (21) and (22). From a computational point of view the proposed theory is simple, since the minimization of the free energy takes only a few seconds with a personal computer.

In section 2 we mentioned that at low densities the MD sampling of the conformational space is not efficient. Because of that the ideal gas populations obtained from MD at low densities present large error bars. To avoid that, a MC integration procedure was developed in order to compute the ideal gas population of the rigid and flexible models. The ideal gas population of the RM and FM are given exactly by equation (4) and equation (10), respectively. We have used a numerical MC procedure in order to evaluate the multidimensional integrals appearing in equation (4) or (10). The procedure for the FM (see equation (10)) is as follows:

(i) The torsional angles of the molecule are randomly chosen. The conformer obtained in this way is classified (for instance, in hexane as the *ttt* conformer).
(ii) The bending angles are generated with a probability proportional to the Boltzmann factor of the bending potential.
(iii) Torsional energy U_{tor}, U_{WCA}, and the metric tensor are evaluated.
(iv) Steps (i)–(iii) are repeated 20×10^6 times so that 20×10^6 different conformers are generated.

The ideal gas population of conformer i is obtained finally as

$$x_i = \frac{\sum_{n_i} \exp\left(-\beta\left(U^{n_i}_{\mathrm{tor}} + U^{n_i}_{\mathrm{WCA}} - 0{\cdot}5kT\ln\left(H^{\mathrm{FM}}_{n_i}\right)\right)\right)}{\sum_{n} \exp\left(-\beta\left(U^{n}_{\mathrm{tor}} + U^{n}_{\mathrm{WCA}} - 0{\cdot}5kT\ln\left(H^{\mathrm{FM}}_{n}\right)\right)\right)}, \tag{23}$$

where the index n runs over all the generated conformers, and n_i is the subset of the generated conformers, classified as conformer i. Approximately half of the generated conformers contribute significantly to the partition function (denominator of equation (23)) so that the number of useful conformers generated is about 10×10^6. This procedure works quite well for short chains like those considered in this work. For longer chains, the algorithm will deteriorate. In that case other methods are available [7]. The uncertainty in the molar fraction of each conformer at zero density obtained in this way is about 0·001. Populations obtained from MC integration were consistent with those obtained from MD at low densities. However, uncertainties are

Table 1. Compressibility factor Z of repulsive n-alkane models. The reduced density is $\rho^* = N/V\sigma^3$ where N is the number of molecules. $Z^{\mathrm{FM}}_{\mathrm{Theory}}$ and $Z^{\mathrm{FM}}_{\mathrm{MD}}$ are the theoretical and simulation results, respectively, for the FM. $Z^{\mathrm{RM}}_{\mathrm{Theory}}$ and $Z^{\mathrm{RM}}_{\mathrm{MD}}$ are the theoretical and simulation results, respectively, for the RM. The simulation results were obtained using the WCA potential.

n[a]	ρ^*	$Z^{\mathrm{FM}}_{\mathrm{Theory}}$	$Z^{\mathrm{RM}}_{\mathrm{Theory}}$	$Z^{\mathrm{FM}}_{\mathrm{MD}}$[b]	$Z^{\mathrm{RM}}_{\mathrm{MD}}$[b]
6	0·118 15	3·04	3·03	3·1(1)	3·1(1)
6	0·200 85	7·10	7·06	7·25(8)	7·31(7)
6	0·295 37	21·02	20·87	20·7(1)	20·8(1)
7	0·100 42	3·09	3·07	3·15(6)	3·13(4)
7	0·177 22	7·79	7·72	8·07(8)	8·00(4)
7	0·254 01	21·66	21·44	21·45(9)	21·50(5)
8	0·088 61	3·20	3·19	3·26(6)	3·26(7)
8	0·153 59	7·85	7·82	8·1(1)	8·09(5)
8	0·224 5	22·88	22·86	23·0(2)	22·97(9)

[a] Number of carbon atoms.

[b] Values in parentheses indicate the uncertainty of the last digit.

dramatically reduced. For the RM we proceed in an analogous way, although step (ii) is removed and H^{RM} replaces H^{FM} in equation (23).

4. Results

In table 1 the simulation results for the EOS of n-hexane, n-heptane and n-octane are presented along with the predictions of the theory described in section 3. The agreement is very good at the lowest and the highest densities and fair at intermediate densities. The theory predicts a different EOS for the RM and for the FM. This is so because the free energy expression (equation (14)) for the RM is slightly different from that of the FM. The conformational equilibrium of the RM and of the FM are different and that affects (although slightly) the EOS. We shall return to this point later. By comparing the simulation results of the RM with those of the FM it may be concluded that angle vibrations hardly affect the EOS of the fluid.

In figure 1 the compressibility factor is plotted as a function of the volume fraction y (the fraction of space occupied by the molecules). Longer molecules present higher values of the compressibility factor at a given volume fraction. That corresponds to the intuitive idea that Z increases with the anisotropy of the molecule for a given value of y. Therefore, long chains present higher anisotropy than short chains.

In table 2, the conformational populations of n-hexane are given at three densities as obtained from the simulations of the RM and of the FM. As mentioned above, for the FM two values of the bending constant k_θ were used. The first thing to be noted is that the conformational populations of the two FMs are almost identical. The value $k_\theta = 520\ \mathrm{kJ\ mol^{-1}}$ is a reasonable approximation to the bending constant of the CCC bond. Therefore, the conformational equilibrium of alkanes is quite close to that of FM with a bending constant going to infinity. This justifies our theoretical treatment of the FM presented in the previous section, where bending vibrations were neglected when computing conformer populations for this model (see equation (13)). The second feature to be noted is that the conformational equilibria of the RM

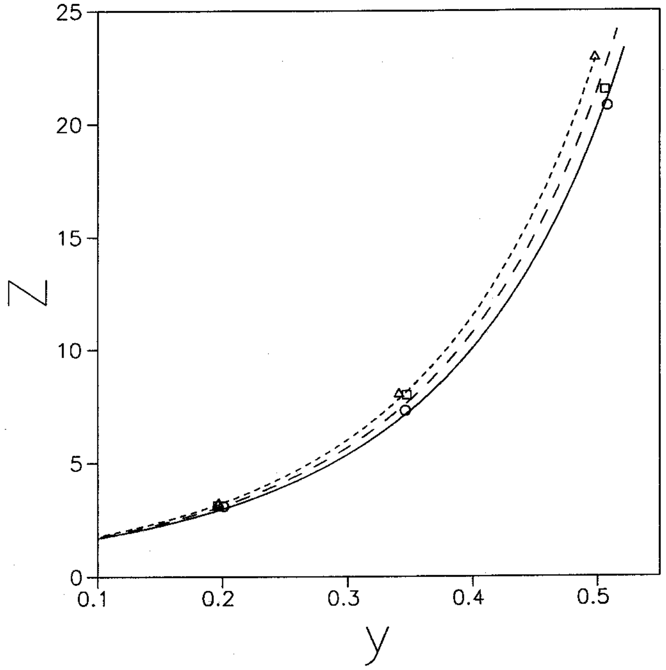

Figure 1. Compressibility factor Z as a function of the packing fraction y defined by equation (18). Symbols represent the MD results of the WCA RM of n-hexane (circles), n-heptane (squares) and n-octane (triangles). The curves correspond to the predictions of the theory described in section 3 for n-hexane (solid curve), n-heptane (dashed curve) and n-octane (short dashed curve).

Table 2. Conformer populations of repulsive models of n-hexane as obtained from MD. The potential used is the WCA. Results are presented for the rigid model (RM) and the flexible model (FM). In the case of the flexible model results are presented for two values of k_θ of equation (1): $k_\theta = 520\ \mathrm{kJ\ mol^{-1}}$ (FM1) and $k_\theta = 1040\ \mathrm{kJ\ mol^{-1}}$ (FM2). In this table, g denotes either a g^+ or a g^- bond. The combination gg' or $g'g$ is not allowed due to the pentane effect (see reference [25]). The reduced density ρ^* is as in table 1. The results for $\rho^* = 0$ were obtained from numerical MC integration. The numbers in parentheses for the MD results show the uncertainty of the last digit. They are given only for the FM1 model to provide an idea of the typical uncertainty. The last row shows the total fraction of *trans* bonds.

	$\rho^* = 0$			$\rho^* = 0{\cdot}118\,15$			$\rho^* = 0{\cdot}295\,37$		
Conformer	FM1	FM2	RM	FM1	FM2	RM	FM1	FM2	RM
ttt	0·276	0·275	0·200	0·27(2)	0·26	0·19	0·22(1)	0·22	0·16
ttg	0·363	0·363	0·361	0·36(2)	0·36	0·36	0·37(1)	0·37	0·36
tgt	0·176	0·177	0·198	0·18(2)	0·18	0·19	0·18(1)	0·19	0·19
tgg	0·059	0·059	0·077	0·069(6)	0·068	0·08	0·067(4)	0·067	0·088
gtg	0·117	0·118	0·154	0·12(1)	0·12	0·16	0·153(9)	0·15	0·19
ggg	0·006	0·006	0·009	0·006(2)	0·008	0·01	0·009(2)	0·010	0·013
t(global)	0·694	0·694	0·649	0·693	0·683	0·637	0·660	0·667	0·619

Table 3. Contribution of the metric tensor term $U_{\mathrm{MT}} = -1/2(\ln(H^{\mathrm{RM}}) - \ln(H_{ttt}^{\mathrm{RM}}))$ and of the WCA potential U_{WCA} to the intramolecular energy for the different conformers of n-hexane. They are evaluated within the rotational isomeric state (RIS) approximation. Energies are given in kT units, with $T = 366{\cdot}88$ K. The metric tensor of the all-*trans* conformer is denoted as H_{ttt}. In the RM, intramolecular energy includes contributions from U_{MT} and from U_{WCA}. In the FM, intramolecular energy includes the term U_{WCA} but not the term U_{MT}.

Conformer	U_{MT}	U_{WCA}
ttt	0	0
ttg	−0·3765	0·0023
tgt	−0·5058	0·0046
tgg	−0·6488	1·4737
gtg	−0·6763	0·0046
ggg	−0·7714	2·9424

and of the FM are different. The RM presents a lower fraction of *trans* bonds with respect to the FM. The use of constraining forces on bending angles affects the conformational equilibrium, and therefore the RM is not equivalent to a FM with its bending constant going to infinity. This has been discussed already in the literature [2, 26, 27]. The origin of this effect is the presence of the metric tensor term H^{RM} in equation (9), which is absent in the corresponding equation of the FM (see equation (13)). In table 3, we show the contributions of the metric tensor term and of the WCA potential to the intramolecular energy as computed for the different conformers of n-hexane within the RIS approximation. It is seen that the metric tensor term favours conformers with *gauche* bonds. This explains the large differences found in the population of the *ttt* conformer for the RM and the FM, presented in table 2. For butane, Almarza *et al.* [2] found that the metric tensor favours the *gauche* conformer over the *trans* conformer. Here, we found that the same conclusion can be drawn for longer chains.

In tables 4 and 5 the conformational equilibrium of n-hexane, as obtained from the theory of this work and from simulation, is presented. Table 4 displays results for

Table 4. Conformer population of a repulsive model of n-hexane. The results labelled as theory correspond to the results of the theory described in section 3. Simulation results for the repulsive WCA model are denoted as MD except at $\rho^* = 0$ where Monte Carlo (MC) integration was used instead. In the simulation, fixed values of bond lengths and bond angles were used (RM).

	ρ^*		$\rho^* = 0{\cdot}118\,15$		$\rho^* = 0{\cdot}295\,37$	
Conformer	Theory	MC	Theory	MD	Theory	MD
ttt	0·195	0·200	0·186	0·19(3)	0·132	0·16(1)
ttg	0·379	0·361	0·378	0·36(3)	0·368	0·360(7)
tgt	0·215	0·198	0·214	0·19(2)	0·206	0·190(8)
tgg	0·038	0·077	0·040	0·08(1)	0·058	0·088(6)
gtg	0·171	0·154	0·179	0·16(1)	0·232	0·19(1)
ggg	0·002	0·009	0·002	0·010(2)	0·003	0·013(2)
t(global)	0·661	0·649	0·654	0·637	0·612	0·619

Table 5. Conformer population of a repulsive model of n-hexane. The results labelled as theory correspond to theoretical predictions from this work. Simulation results for the repulsive WCA model are denoted as MD. In the simulations the FM1 (see table 2) was used.

	ρ^*		$\rho^* = 0{\cdot}118\,15$		$\rho^* = 0{\cdot}295\,37$	
Conformer	Theory	MC	Theory	MD	Theory	MD
ttt	0·282	0·276	0·271	0·27(2)	0·201	0·22(1)
ttg	0·376	0·363	0·378	0·36(2)	0·378	0·37(1)
tgt	0·187	0·176	0·188	0·18(2)	0·187	0·18(1)
tgg	0·029	0·059	0·031	0·069(6)	0·046	0·067(4)
gtg	0·125	0·117	0·133	0·12(1)	0·186	0·153(9)
ggg	0·001	0·006	0·001	0·006(2)	0·003	0·009(2)
t(global)	0·708	0·694	0·702	0·693	0·655	0·660

the RM and Table 5 the results for the FM. For most of the conformers, the theory predicts correctly the change in population due to packing effects, and in many cases the predictions are within the uncertainty of the simulation results. At low densities the small disagreement between theory and simulation is due to the use of the RIS approximation, since this is the only approximation used in the theoretical treatment. The ideal gas population of the *tgg* and *ggg* conformers is underpredicted by the theory. This is a consequence of the high value of U_{WCA} in these conformers (see table 3), owing to a small overlap between sites. It should be recalled that, in the context of the RIS approximation, the *tgg* conformer is defined by $\phi_1 = 0$, $\phi_2 = 2\pi/3$, $\phi_3 = 2\pi/3$. If we permit slightly different values of these torsion angles the U_{WCA} energy decreases substantially. As a matter of fact, fluctuations in the torsion angles are allowed in the simulations. In the theory, however, we are using the RIS approximation where no fluctuations are included. For most of the conformers, these fluctuations do not change the U_{WCA} energy substantially. But, when a sequence with several *gauche* bonds is involved, these fluctuations alter the U_{WCA} energy significantly. This explains why the RIS fails in conformers involving a sequence of *gauche* bonds (*tgg* and *ggg* in n-hexane).

In tables 6 and 7 the conformational equilibria of n-heptane, as determined from theory and from simulation, are presented. Table 6 contains the results for the RM, and Table 7 those for the FM. The agreement between theory and simulation is quite good, and the discrepancies are similar to those explained in the case of hexane. In general, theoretical results for the FM show better agreement with the simulation than do those for the RM. This is so because the use of the RIS approximation in the FM affects only the U_{WCA} term, whereas in the RM it affects both the U_{WCA} and the metric tensor term. Nevertheless, the overall agreement between theory and simulation is good.

The results for the RM of octane are presented in table 8, which illustrates how the theory can be implemented for longer chains. The only requirement to apply the theory to these chains is the knowledge of the volume and the second virial coefficient of each conformer. Good and fast algorithms are already available for computing analytically the volume of any conformer [29]. In this work, we have used the second virial coefficients numerically computed in previous work [19]. This numerical determination is time consuming, and therefore it would be very useful to have a

Table 6. Conformer population of a repulsive model of n-heptane. Notation as in table 4. MD results correspond to the rigid model (RM).

	$\rho^* = 0$		$\rho^* = 0{\cdot}10042$		$\rho^* = 0{\cdot}25401$	
Conformer	Theory	MC	Theory	MD	Theory	MD
tttt	0·105	0·113	0·098	0·11(1)	0·063	0·088(7)
tttg	0·217	0·211	0·213	0·21(1)	0·183	0·20(1)
ttgt	0·268	0·242	0·264	0·24(2)	0·230	0·217(9)
ttgg	0·024	0·048	0·025	0·047(8)	0·031	0·047(4)
tgtg	0·242	0·208	0·249	0·21(1)	0·289	0·24(1)
tggt	0·014	0·026	0·014	0·028(7)	0·018	0·027(5)
gttg	0·106	0·095	0·110	0·10(2)	0·136	0·110(9)
tggg	0·002	0·012	0·003	0·012(3)	0·004	0·016(2)
gtgg	0·021	0·040	0·024	0·044(5)	0·044	0·056(8)
gggg	0·0001	0·001	0·0001	0·002(1)	0·0003	0·003(1)
t(global)	0·670	0·654	0·664	0·654	0·627	0·630

Table 7. Conformer population of a repulsive model of n-heptane. Notation as in table 4. MD results correspond to the flexible model (FM).

	$\rho^* = 0$		$\rho^* = 0{\cdot}10042$		$\rho^* = 0{\cdot}25401$	
Conformer	Theory	MC	Theory	MD	Theory	MD
tttt	0·191	0·185	0·180	0·18(1)	0·123	0·15(1)
tttg	0·255	0·245	0·253	0·25(1)	0·233	0·233(7)
ttgt	0·255	0·238	0·253	0·23(1)	0·234	0·23(1)
ttgg	0·020	0·040	0·021	0·041(4)	0·028	0·043(4)
tgtg	0·170	0·154	0·176	0·15(1)	0·218	0·18(1)
tggt	0·010	0·020	0·010	0·021(4)	0·014	0·022(4)
gttg	0·085	0·080	0·089	0·084(6)	0·117	0·094(9)
tggg	0·002	0·008	0·002	0·010(2)	0·003	0·011(2)
gtgg	0·013	0·026	0·015	0·028(5)	0·028	0·035(4)
gggg	0·00006	0·0008	0·00007	0·0014(8)	0·0002	0·0014(8)
t(global)	0·721	0·703	0·714	0·698	0·673	0·678

faster procedure for estimating the second virial coefficient of each hard conformer. This work shows that such an effort would be worthwhile since, if this were achieved, the theory presented in section 3 would be a simple method for providing good results for the EOS and the conformational equilibrium of chain molecules.

The physical picture emerging from the results displayed in Tables 4–8 is as follows. At liquid densities, the populations of the more anisotropic conformers decrease with respect to that of the gas phase. On the other hand, the more spherical conformers increase their populations at liquid densities with respect to the gas phase. Following Rigby [28], we use the non-sphericity parameter α as a quantitative measure of the anisotropy of a hard model. Equation (20) defines the non-sphericity parameter α_i of a given conformer. We use α_i as a measure of the anisotropy of a given conformer i. For a spherical molecule $\alpha = 1$, whereas for an anisotropic model the value of α is always larger than one. According to the theoretical treatment of [19], a drop in the population of conformers with large α (strongly anisotropic)

Table 8. Conformer population of a repulsive model of n-octane. Notation as in table 4. MD results were obtained for the rigid model (RM).

	$\rho^* = 0$		$\rho^* = 0{\cdot}2245$	
Conformal	Theory	MC	Theory	MD
ttttt	0·0552	0·063	0·029	0·048(5)
ttttg	0·119	0·119	0·091	0·107(9)
tttgt	0·156	0·141	0·120	0·119(8)
ttgtt	0·086	0·075	0·067	0·065(6)
tttgg	0·014	0·028	0·016	0·026(3)
ttggt	0·017	0·032	0·022	0·034(3)
gtttg	0·062	0·056	0·065	0·062(4)
gttgt	0·154	0·129	0·177	0·130(10)
gtgtt	0·155	0·129	0·166	0·138(12)
tgtgt	0·088	0·069	0·093	0·075(7)
gggtt	0·001	0·007	0·002	0·009(3)
ggttg	0·014	0·024	0·002	0·027(3)
tgggt	0·0009	0·004	0·001	0·005(2)
tggtg	0·0038	0·027	0·007	0·032(4)
tgtgg	0·0038	0·027	0·007	0·035(4)
gtgtg	0·070	0·054	0·105	0·073(9)
ggggt	0·0001	0·002	0·0003	0·003(1)
gggtg	0·0014	0·006	0·003	0·010(2)
ggtgg	0·0005	0·002	0·002	0·004(1)
ggggg	0·000006	0·0002	0·00002	0·0004(2)
t(global)	0·675	0·656	0·636	0·635

decreases the configurational free energy of the system. Since the system at equilibrium tends to its free energy minimum, the population of such conformers decreases at liquid densities. These predictions agree with the simulation results presented in tables 4–8. For each n-alkane model, an average anisotropy α can be defined. This average anisotropy is obtained through a weighted average (see equation (19)) of the anisotropy of the different conformers present in the n-alkane fluid. As a general rule, a conformer labelled as i with $\alpha_i > \alpha$ will decrease its population as the density increases. Conversely, if $\alpha_i < \alpha$ then the population of conformer i will increase as the density increases. Conformers with many *trans* bonds tend to have higher values of the second virial coefficient, and therefore higher values of α (see [19]). All this can be summarized by saying that conformers with a higher fraction of *trans* bonds present a large anisotropy. Therefore, the packing effects will reduce the population of conformers with many *trans* bonds. Hence, the total fraction of *trans* bonds will decrease as the density increases. This is shown explicitly in table 9, where the drop of *trans* population of the WCA models of n-alkanes is presented for n-hexane, n-heptane and n-octane. Both theory and simulation show a decrease in the total fraction of *trans* bonds, due to packing effects. This is true for the RM as well as for the FM. For the range of densities considered, the fraction of *trans* bonds is reduced on average by about 3%. The theory predicts a decrease on average of about 5%, which is in good agreement with the simulation results taking into account that the uncertainty of the MD results is about 1%. These results are in agreement with previous results for butane [2, 4, 5, 7]. At high densities, the theory slightly

Table 9. Shift with density of the population of *trans* bonds for the WCA and LJ models of n-alkanes. Results are presented for the RM and FM (FM1) as obtained from MD simulations and from theory. Δ is defined as the percentage difference of the population of *trans* bonds at the highest considered density and at zero density. The highest considered density for each alkane is shown in table 1

n^a	Potential	Model	Method	Δ
6	WCA	RM	Theory	−4·9
6	WCA	RM	MD	−3
6	WCA	FM	Theory	−5·3
6	WCA	FM	MD	−3·4
7	WCA	RM	Theory	−4·3
7	WCA	RM	MD	−2·4
7	WCA	FM	Theory	−4·8
7	WCA	FM	MD	−2·5
8	WCA	RM	Theory	−3·9
8	WCA	RM	MD	−2·1
6	LJ	RM	MD	+0·5
7	LJ	RM	MD	+0·9

[a]Number of carbon atoms.

overestimates the effect of packing on conformational equilibrium. In fact, the decrease of the *trans* population is more pronounced in theory than in simulation.

The results presented so far correspond to purely repulsive models of n-alkanes. In order to understand the role of attractive forces on the conformational equilibrium, we have performed a few simulations for n-hexane and n-heptane, with the model as described, but with the potential energy of equations 2 and 3 replaced by the full Lennard-Jones (LJ) potential:

$$u^{\mathrm{LJ}} = 4\epsilon\left(\left(\frac{\sigma}{r}\right)^{12} - \left(\frac{\sigma}{r}\right)^{6}\right). \tag{24}$$

The pair interaction is truncated at $r_c = 2{\cdot}5\sigma$. Long tail corrections to the pressure were computed by using the procedure proposed by Toxvaerd [30]. Our simulations of the LJ models were performed with the RM. For each n-alkane, three densities were studied, corresponding to those previously considered for the WCA models (see tables 4 and 6). Let us mention that, for the intermediate density, the pressure was found to be negative both in the LJ model of n-hexane and in the LJ model of n-heptane. This is an indication of a metastable state within the two phases coexistence region. At the intermediate densities ($\rho^* = 0{\cdot}118\,15$ and $\rho^* = 0{\cdot}100\,42$) the LJ models are probably in the two phase coexistence region.

The conformational population for the LJ model of n-hexane is presented in table 10, along with the results of the WCA rigid model. The results for the LJ model of n-heptane and for the corresponding WCA model are presented in table 11. At low densities ($\rho^* = 0$) the conformational equilibria of the WCA and the LJ model are slightly different. The WCA model presents a higher fraction of *trans* bonds. This is so because conformations in which the molecule adopts a globular shape are favoured in the LJ model due to the attractive nature of the LJ potential. Since conformations presenting several *gauche* bonds present a globular shape, the LJ potential favours

Table 10. Conformer population for the WCA model of n-hexane and for the full LJ model of n-hexane. MD results for the repulsive WCA model are denoted as WCA. MD results for the full LJ potential are denoted as LJ. Results at zero density were obtained by Monte Carlo integration. In all these simulations, fixed values of bond lengths and bond angles were used (RM).

	$\rho^* = 0$		$\rho^* = 0{\cdot}118\,15$		$\rho^* = 0{\cdot}295\,37$	
Conformer	WCA	LJ	WCA	LJ	WCA	LJ
ttt	0·200	0·179	0·19(3)	0·19	0·16(1)	0·182
ttg	0·361	0·360	0·36(3)	0·35	0·360(7)	0·361
tgt	0·198	0·198	0·19(2)	0·21	0·190(8)	0·204
tgg	0·077	0·083	0·08(1)	0·080	0·088(6)	0·079
gtg	0·154	0·168	0·16(1)	0·163	0·19(1)	0·164
ggg	0·009	0·009	0·010(2)	0·009	0·013(2)	0·010
t(global)	0·649	0·635	0·637	0·643	0·619	0·640

Table 11. As for table 10, but for n-heptane.

	$\rho^* = 0$		$\rho^* = 0{\cdot}100\,42$		$\rho^* = 0{\cdot}254\,01$	
Conformer	WCA	LJ	WCA	LJ	WCA	LJ
tttt	0·113	0·093	0·11(1)	0·109	0·088(7)	0·100
tttg	0·211	0·192	0·21(1)	0·203	0·20(1)	0·201
ttgt	0·242	0·238	0·24(2)	0·247	0·217(9)	0·244
ttgg	0·048	0·050	0·047(8)	0·047	0·047(4)	0·045
tgtg	0·208	0·222	0·21(1)	0·229	0·24(1)	0·224
tggt	0·026	0·031	0·028(7)	0·026	0·027(5)	0·026
gttg	0·095	0·104	0·10(2)	0·086	0·110(9)	0·098
tggg	0·012	0·014	0·012(3)	0·012	0·016(2)	0·015
gtgg	0·040	0·049	0·044(5)	0·040	0·055(8)	0·045
gggg	0·001	0·001	0·002(1)	0·001	0·003(1)	0·001
t(global)	0·654	0·636	0·654	0·654	0·630	0·645

conformers with several *gauche* bonds. As a consequence, at zero density the total fraction of *trans* bonds is lower in the LJ model with respect to the WCA model. This is true for n-hexane and n-heptane. We conclude that intramolecular attractive forces favour conformers with several *gauche* bonds. Although this is an interesting result, in this work we focus on the effect of intermolecular forces on the conformational equilibria. Therefore the effect of density on the conformational equilibria should be analysed, rather than differences at zero density. Differences at high densities between the conformational populations of the WCA and the LJ models are clearly visible. In the WCA model, populations of conformers with many *trans* bonds decrease as the density increases. Therefore, a decrease in the total fraction of *trans* bonds is observed (see last rows of tables 10 and 11). However, for the LJ model the populations of conformers with many *trans* bonds increase with the density. Thus, the total fraction of *trans* bonds increases with the density, although the effect is small. This is illustrated further in table 9, where the effect of density on the total fraction of *trans* bonds is shown. The LJ models present positive values of Δ, whereas the WCA models have negative values. Our results for the LJ model are in agreement with those of Almarza *et al.* [3]. In fact, these authors found a slight increase of *trans* population with density in a LJ model of n-hexane.

The data in tables 10 and 11 suggest that intermolecular attractive forces play a role in the conformational equilibrium of n-alkanes. Intermolecular attractive forces seem to favour the more anisotropic conformers (i.e., conformers with many *trans* bonds) over the more spherical ones. That would explain why the global *trans* population in the WCA model decreases with density, whereas it slightly increases in the LJ model. This is in agreement with previous findings for butane [2].

5. Conclusion

Molecular dynamics simulations of purely repulsive n-alkane models have been performed. The results were used to test an equation of state recently proposed for hard n-alkane models. Good agreement between theory and simulation has been found for the equation of state. Bending vibrations hardly affect the equation of state.

The conformational equilibrium of models with holonomic constraints in bond angles is different from that of flexible models, even if the bending constant is set to an arbitrarily high value. The population of *trans* conformers in the rigid model is systematically smaller than in the flexible model, where bond angle vibrations are allowed. The explanation of that arises from the fact that the metric tensor favours *gauche* bonds. When one develops theories to describe the effect of packing on the conformational equilibrium, it should be remembered that different treatments are needed in order to compare with the simulation results obtained from the RM or from the FM.

The conformational equilibrium has been analysed for different chain lengths at several densities. In repulsive n-alkane models, the packing effects result in an increase of the population of the more spherical conformers over the more anisotropic ones. Since the more spherical conformers present a large number of *gauche* bonds, there is a growth in the *gauche* population when density increases. This is in agreement with the predictions of [19]. On the other hand, intermolecular attractive forces affect the conformational equilibrium by favouring the more anisotropic conformers (large number of *trans* bonds) over the more spherical ones. Thus, repulsive and attractive intermolecular forces favour different kinds of conformers at liquid densities. It is likely that at very high densities repulsive forces will dominate the conformational equilibrium. However, at common liquid densities the effects of repulsive and attractive forces on the conformational equilibrium approximately cancel out. This explains why the conformational equilibrium of short chains at liquid densities is very close to that of the gas at the same temperature. This work suggests that the effects of repulsive and attractive forces on the conformational equilibrium cancel out at moderate liquid densities.

This work has been supported financially by Grant No. 11-0065-1 from the Danish Natural Science Research Council and by the Project PB91-0364 of the Spanish DGICYT (Dirección General de Investigación Científica y Técnica). One of us (P.P.) wishes to gratefully acknowledge EEC Grant No. ERBCHBICT930394 for financial support. We thank Søren Toxvaerd, Eduardo Enciso and Noe G. Almarza for helpful discussions.

References

[1] RYCKAERT, J. P., and BELLEMANS, A., 1978, *J. chem. Soc. Faraday Discuss.*, **66**, 95.
[2] ALMARZA, N. G., ENCISO, E., ALONSO, J., BERMEJO, F. J., and ALVAREZ, M., 1990, *Molec. Phys.*, **70**, 485.
[3] ALMARZA, N. G., ENCISO, E., and BERMEJO, F. J., 1989, *J. chem. Phys.*, **90**, 413.
[4] ELLIOTT, J. R., and KANETKAR, U. S., 1990, *Molec. Phys.*, **71**, 871.
[5] ELLIOTT, J. R., KANETKAR, U. S., and VASUDEVAN, V. J., 1990, *Molec. Phys.*, **71**, 883.
[6] BROWN, D., and CLARKE, J. H. R., 1990, *J. chem. Phys.*, **92**, 3062.
[7] BROWN, D., CLARKE, J. H. R., OKUDA, M., and YAMAZAKI, T., 1994, *J. chem. Phys.*, **100**, 1684.
[8] PADILLA, P., and TOXVAERD, S., 1991, *J. chem. Phys.*, **94**, 5650.
[9] PADILLA, P., and TOXVAERD, S., 1991, *J. chem. Phys.*, **95**, 509.
[10] YETHIRAJ, A., CURRO, J. G., SCHWEIZER, K. S., and MCCOY, J. D., 1993, *J. chem. Phys.*, **98**, 1635.
[11] DICKMAN, R., and HALL, C. K., 1988, *J. chem. Phys.*, **89**, 3168.
[12] KIERLIK, E., and ROSINBERG, M. L., 1992, *J. chem. Phys.*, **97**, 9222.
[13] KIERLIK, E., and ROSINBERG, M. L., 1993, *J. chem. Phys.*, **99**, 3950.
[14] WERTHEIM, M. S., 1987, *J. chem. Phys.*, **87**, 7323.
[15] CHAPMAN, W. G., JACKSON, G., and GUBBINS, K. E., 1988, *Molec. Phys.*, **65**, 1057.
[16] AMOS, M. D., and JACKSON, G., 1992, *J. chem. Phys.*, **96**, 4604.
[17] HONNELL, K. G., and HALL, C. K., 1989, *J. chem. Phys.*, **90**, 1841.
[18] BOUBLÍK, T., VEGA C., and PEÑA, M. D., 1990, *J. chem. Phys.*, **93**, 730.
[19] VEGA, C., LAGO, S., and GARZON, B., 1994, *J. chem. Phys.*, **100**, 2182.
[20] EDBERG, R., EVANS, D. J., and MORRIS, G. P., 1986, *J. chem. Phys.*, **84**, 6933.
[21] WEEKS, J. D., CHANDLER, D., and ANDERSEN, H. C., 1971, *J. chem. Phys.*, **54**, 5237.
[22] BARKER, J. A., and HENDERSON, D., 1976, *Rev. mod. Phys.*, **48**, 587.
[23] See for example, Nosé, S., 1991, *Progress of Theoretical Physics*, Supplement No. 103, p. 1.
[24] TOXVAERD, S., 1991, *Molec. Phys.*, **72**, 159.
[25] FLORY, P. J., 1969, *Statistical Mechanics of Chain Molecules* (New York: Wiley).
[26] VAN GUNSTEREN, W. F., 1980, *Molec. Phys.*, **40**, 1015.
[27] RYCKAERT, J. P., 1991, *Computer Simulation in Materials Science*, edited by M. Meyer and V. Pontikis (Dordrecht: Kluwer).
[28] RIGBY, M., 1976, *Molec. Phys.*, **32**, 575.
[29] DODD, L. R., and THEODOROU, D. N., 1991, *Molec. Phys.*, **72**, 1313.
[30] TOXVAERD, S., 1988, *J. chem. Phys.*, **89**, 3808.